14454 *J. Phys. Chem. C* **2009,** *113,* 14454–14466

Effect of Al/Si Substitutions and Silanol Nests on the Local Geometry of Si and Al Framework Sites in Silicone-Rich Zeolites: A Combined High Resolution ^{27}Al and ^{29}Si NMR and Density Functional Theory/Molecular Mechanics Study

Jiří Dědeček,[†] Stepan Sklenak,*,[†] Chengbin Li,[†] Fei Gao,[†] Jiří Brus,[‡] Qingjun Zhu,[§,⊥] and Takashi Tatsumi[§]

J. Heyrovský Institute of Physical Chemistry, Academy of Sciences of the Czech Republic, Dolejškova 3, 182 23 Prague, Czech Republic, Institute of Macromolecular Chemistry of the Academy of Sciences of the Czech Republic, Heyrovsky Square 2, 162 06 Prague 6, Czech Republic, and Chemical Resources Laboratory, Tokyo Institute of Technology, 4259 Nagatsuta-cho, Midori-ku, Yokohama 226-8503, Japan

Received: May 6, 2009; Revised Manuscript Received: June 8, 2009

We employed ^{29}Si and ^{27}Al (3Q) magic-angle spinning (MAS) NMR spectroscopy and density functional theory/molecular mechanics (DFT/MM) calculations to investigate the effect of Al/Si substitutions and the presence of silanol nests on the ^{29}Si and ^{27}Al NMR parameters as well as the local geometry of SiO_4 and AlO_4^- tetrahedra of the nearest and next-nearest neighboring Si and Al atoms. The silicon-rich zeolite of the chabazite structure (Si/Al 38) was chosen for this study as a representative model of silicon-rich zeolites since it exhibits a low number of distinguishable T sites. Our computational results show the following: (I) Al atoms can occupy three different crystallographic T sites in the framework of chabazite (Si/Al 38). This result is in agreement with two observed ^{27}Al NMR resonances. (II) An Al/Si substitution causes a downshift of the ^{29}Si chemical shift of the nearest neighboring *Si* atoms (Al−O−*Si*) by 4−11 ppm. (III) The effect of a more distant Al/Si substitution (Al−O−Si−O−*Si*) is significantly less pronounced (downshift up to 2 ppm). (IV) An Al/Si substitution (Al−O−Si−O−*Al*) leads to larger ^{27}Al isotropic chemical shifts of the next-nearest neighboring *Al* atoms by up to 3 ppm. (V) The presence of a silanol “nest” (vacant T site) as a nearest (H−O−*Si*) and next-nearest (H−O−Si−O−*Si*) neighbor is responsible for a systematic downshift of the ^{29}Si chemical shift of Si by 11−16 ppm and by 0−1 ppm, respectively. (VI) There is no systematic effect of a silanol “nest” as a next-nearest neighbor (H−O−Si−O−*Al*) on the ^{27}Al isotropic chemical shift of Al as its values are smaller for some H−O−Si−O−*Al* sequences (up to −3.6 ppm) and greater for others (up to +2.9 ppm). (VII) Al atoms present in hypothetical Al−O−Al sequences would have their ^{27}Al isotropic chemical shifts larger by 7−9 ppm than single Al atoms. Our predictions of NMR parameters using the quantum mechanics/interatomic potential functions approach and our bare zeolite framework model are in good agreement with the available experiments.

1. Introduction

Zeolites are crystalline, microporous aluminosilicates $[Si_{n-m}Al_mO_{2n}]^{m-}$ made of corner-sharing TO_4 tetrahedra (T = Si, Al^-). They are widely used as catalysts and adsorbents in industrial chemical processes exploiting their site specificity and properties of molecular sieves. In the past thirty years, attention was mainly drawn to silicon-rich zeolites (with Si/Al > 12). Their protonic forms are currently used as acid catalysts for selective hydrocarbon synthesis and transformations in petrochemistry.[1] Their transition-metal exchanged forms have been discovered as exceptional redox catalysts.[2−4]

The species assumed to be the active sites in the mentioned reactions, that is, protons, metal ions, and metal−oxo species, are positively charged and compensate the negatively charged AlO_4^- tetrahedra. The local structures of these AlO_4^- tetrahedra therefore influence the structure and properties of the active sites. In addition, since the local geometry of AlO_4^- tetrahedra significantly differs from that of SiO_4 tetrahedra because of the elongation of Al−O bonds with respect to Si−O ones by some 0.13 Å, each Al/Si substitution significantly perturbs the ideal structure of the all-silica zeolite framework. The four nearest neighboring SiO_4 tetrahedra are affected the most, but also the next-nearest neighboring SiO_4 tetrahedra are influenced by that Al/Si substitution.[5]

The local structure of AlO_4^- tetrahedra in frameworks of silicon-rich materials as well as SiO_4 tetrahedra that are the nearest and next-nearest neighbors of these AlO_4^- tetrahedra cannot be studied by diffraction techniques because of the low concentration of framework Al atoms in these materials, the low symmetry of the unit cell, and a high number of framework T sites. On the other hand, high resolution ^{27}Al multiple-quantum (MQ) and ^{29}Si magic-angle spinning (MAS) NMR spectroscopies represent powerful tools to characterize the local structures of AlO_4^- and SiO_4, respectively, in zeolite frameworks.[6,7] However, interpretations of ^{29}Si and ^{27}Al NMR experiments are only empirical. Linear correlations between the ^{29}Si chemical shift and the ^{27}Al isotropic chemical shift and the average Si−O−Si[8−10] and the T−O−T[11]

---

[*] Corresponding author. E-mail: stepan.sklenak@jh-inst.cas.cz.

[†] J. Heyrovsky Institute of Physical Chemistry, Academy of Sciences of the Czech Republic.

[‡] Institute of Macromolecular Chemistry of the Academy of Sciences of the Czech Republic.

[§] Tokyo Institute of Technology.

[⊥] Present address: Department of Chemistry, Northwestern University, Evanston, IL 60208, U.S.A.

10.1021/jp9042232 CCC: $40.75

angles, respectively, were suggested. There is no empirical correlation between the structural parameters and the corresponding ^{29}Si NMR parameters available in the literature for Si atoms with Al atoms or silanol (OH) groups as nearest neighbors. There are only known ranges of the ^{29}Si chemical shift for framework Si atoms possessing a different number of Al atoms as next neighbors (i.e., Si(3Si,1Al), Si(2Si,2Al), Si(1Si,3Al), and Si(0Si,4Al)), and similarly, there are published ranges of the ^{29}Si chemical shift for framework Si(3Si,OH) atoms for different zeolite frameworks.[7,12,13] These empirical and rough estimates of the ^{29}Si chemical shifts are employed to characterize zeolite materials. They allow (I) the calculation of the concentration of Al atoms in the framework,[12] (II) the estimation of the Al distribution in Al-rich zeolites,[7,12,14] and (III) the investigation of the dealumination of zeolite frameworks.[15−17] It should be noted that the rules and relations applied to interpret the relation between the ^{29}Si chemical shift and the corresponding Si−Al ordering[5] in the zeolite framework were established experimentally for the faujasite zeolite (one framework T site and a Si/Al ratio usually smaller than three). Therefore, it is obvious that a more detailed knowledge of the relationship between the ^{29}Si chemical shift and the ^{27}Al isotropic chemical shift of framework Si and Al atoms, respectively, and the local geometry of SiO_4 and AlO_4^- tetrahedra, respectively, is needed, especially for the interpretation of experimental results obtained for silicon-rich matrices. To achieve this, a knowledge of the effects of Al atoms and silanol groups (OH) as nearest and next-nearest neighbors (the two most common defects in the ideal all-silica framework structure) on the local geometry of SiO_4 and AlO_4^- tetrahedra of silicon-rich zeolites is necessary.

Progress in computational chemistry permitted calculating reasonable zeolite structures as well as NMR parameters. Sauer et al., employing the gauge-invariant atomic orbital/coupled perturbed Hartree−Fock (GIAO−CPHF) method,[18] obtained the ^{29}Si chemical shifts of all-silica zeolite structures which were in good agreement with the observed chemical shifts.[19] The agreement was slightly better for structures optimized with an ab initio parametrized force field[20] than those having the experimental X-ray geometries. The calculations yielded the correct order of all 12 observed ^{29}Si NMR resonances for the orthorhombic structure of the ZSM-5 zeolite.[19] Bull et al. evaluated ^{17}O isotropic chemical shifts and electric-field gradients of oxygen in siliceous faujasite and ferrierite[21,22] employing the GIAO−CPHF method. A complete assignment of the four observed lines for faujasite was obtained, while only a partial assignment was achieved for ferrierite. Periodic density functional theory (DFT) calculations brought some improvement but did not change the sequence of signals for the different positions.[23] Kučera and Nachtigall[24] studied the MCM-58 zeolite by periodic DFT. They found that the GIAO NMR shielding of Al in the framework dramatically varies with the coordination of the countercation in the cationic site and with the number of water molecules coordinated to the countercation.

Recently, a combined approach employing ^{27}Al MQ MAS NMR spectroscopy together with quantum mechanics (QM) and molecular mechanics (MM) calculations was successfully employed to describe the geometry of AlO_4^- tetrahedra in the framework of the ZSM-5 zeolite and to determine a partial site of Al atoms in the individual framework T sites.[25,26] In addition, the effect of an Al atom as a next-nearest (Al−O−Si−O−Al) and next-next-nearest (Al−O−Si−O−Si−O−Al) neighbor on the ^{27}Al NMR parameters and the local geometry of AlO_4^- tetrahedra was investigated employing the combined approach.[27]

In this paper, employing QM/MM calculations together with our bare zeolite framework model[25−28] in a combination with high resolution multinuclear NMR experiments, we investigate the effect of an **Al** atom as a nearest (**Al**−O−*Si* and hypothetical **Al**−O−*Al*[29]) and next-nearest (**Al**−O−Si−O−*Si* and **Al**−O−Si−O−*Al*) neighbor on the ^{29}Si chemical and ^{27}Al isotropic chemical shift of *Si* and *Al*, respectively, and the local geometry of *Si*O$_4$ and *Al*O$_4^-$ tetrahedra, respectively, in frameworks of silicon-rich zeolites. In addition, the effect of a silanol "nest" as a nearest (H−O−*Si*) and next-nearest (H−O−Si−O−*Si* and H−O−Si−O−*Al*) neighbor is investigated as well.

The silicon-rich zeolite of the chabazite structure was chosen for this study as a representative model of silicon-rich zeolites. Chabazite has a simple structure for its unit cell, possessing one distinguishable T site for Al-rich[30] frameworks. Therefore, the chabazite structure is a suitable, and simple, model system for study of (I) SiO_4 and AlO_4^- in silicon-rich zeolites and (II) the effect of an Al/Si substitution on the number of distinguishable T sites in the framework. The results of our quantum mechanics/interatomic potential functions (QM-Pot) calculations were compared with our results of ^{29}Si and ^{27}Al (MQ) MAS NMR experiments on a silicon-rich chabazite H−CHA (Si/Al 38) sample.

2. Experimental Section

2.1. Sample. Silicon-rich chabazite H−CHA (Si/Al 38) was prepared by using TMAdaOH as a structure-directing agent according to ref 31. A detailed description of the synthesis is given in refs 32 and 33. A fully hydrated H−CHA sample was used in our NMR experiments. X-ray diffraction and scanning electron microscopy indicated good crystallinity of the calcined sample. Moreover, ^{27}Al and ^{29}Si MAS NMR showed no detectable extra-framework Al atoms.

2.2. MAS NMR Spectroscopy. ^{29}Si and ^{27}Al MAS NMR as well as ^{27}Al 3Q MAS NMR experiments were carried out on a Bruker Avance 500 MHz (11.7 T) Wide Bore spectrometer using 4 mm outside diameter ZrO_2 rotors with a rotation speed of 5 kHz for ^{29}Si MAS NMR and 12 kHz for ^{27}Al MAS NMR. For the ^{29}Si MAS NMR high-power decoupling experiment, a $\pi/6$ (1.7 μs) excitation pulse, relaxation delay of 30 s, and 50% ramp cross-polarization (CP) pulse sequence were applied to collect a single pulse and CP spectra. The ^{29}Si chemical shifts were referenced to Q8M8. The content of the framework aluminum (Si/Al$_{FR}$) was estimated from the ^{29}Si NMR data using[12]

$$\mathrm{Si/Al_{FR}} = I/\sum 0.25 n I_n \tag{1}$$

where I denotes the total intensity of the ^{29}Si NMR signal in the single pulse experiment and I_n denotes the intensity of the NMR signal corresponding to the Si(4-nSi,nAl) atoms.

To allow a quantitative evolution of the ^{27}Al MAS NMR spectra, high-power decoupling pulse sequences with a $\pi/12$ (0.7 μs) excitation pulse were applied. The chemical shifts were referenced to the aqueous solution of Al(NO$_3$)$_3$. Two-dimensional multiquantum experiments (2D 3Q) were used to determine the ^{27}Al isotropic chemical shift, δ_{iso} ^{27}Al. The 3Q experiments were performed using the z-filtered procedure. A $\pi/2$ pulse was used for the excitation and a $\pi/3$ pulse for the conversion. The pulses were individually optimized for each sample. The 2D contour plots are the results of a 2D Fourier transformation followed by a shearing transformation. The isotropic chemical shift was estimated using

$$\delta_{iso} = (17\delta_{F1} + 10\delta_{F2})/27 \tag{2}$$

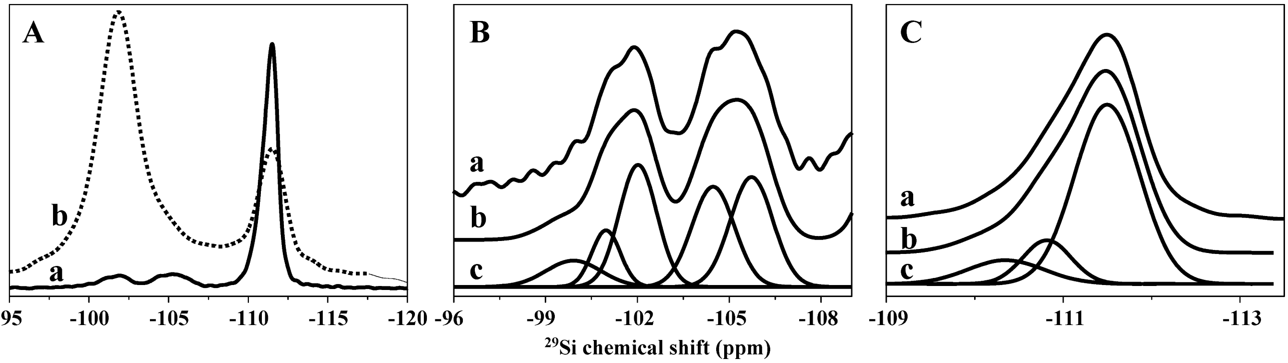

Figure 1. ^{29}Si single pulse (a) and CP (b) MAS NMR spectra of the silicon-rich chabasite (A). Analysis of the ^{29}Si single pulse MAS NMR spectra in the region of Si(3Si,OH) and Si(3Si,1Al) atoms (B) and in the region of Si(4Si) atoms (C). Experimental spectrum (a), spectrum simulation (b), and individual Gaussian bands of the spectra simulation (c).

where δ_{F1} is the chemical shift in the isotropic and δ_{F2} in the observed dimensions. The ^{27}Al 3Q MAS NMR spectroscopy of silicon-rich zeolites is discussed by van Bokhoven et al.,[6] and the 3Q MAS NMR technique is explained in detail by Alemany.[34]

3. Experimental Results

^{29}Si and ^{29}Si CP MAS NMR spectra are depicted in Figure 1. The asymmetric band around −112 ppm can be attributed to the Si(4Si) atoms.[7,12] Note that the asymmetry of the band indicates that this signal corresponds to at least two close resonances. The simulation of the spectra using Gaussian bands is evidence of the presence of three resonances at −111.5 (strong), −110.8 (weak), and −110.3 (weak) ppm. The weak, broad, and complex bands at around −106 and −102 ppm reflect Si(3Si,1Al) and/or Si(3Si,OH) atoms.[7] The results of our CP experiment (Figure 1) indicate that the signal at about −106 ppm corresponds to the Si(3Si,1Al) atoms, while the band at around −102 ppm relates to Si(3Si,OH) species. Our simulation of the spectra indicates that the band at −102 ppm reflects three resonances centered at −99.9, −101.0, and −102.0 ppm, while the signal at −106 ppm is composed of two resonances centered at −104.5 and −105.7 ppm.

The silicon to framework aluminum ratio of the sample (Si/Al$_{FR}$, 40) estimated using eq 1 is in good agreement with the Si/Al value of 38 obtained from chemical analysis. This indicates that aluminum atoms are exclusively present in the zeolite framework.

2D projection of the ^{27}Al 3Q MAS NMR experiment together with the F1 projection and its simulations are given in Figure 2. The effect of the quadrupolar interaction is removed in the F1 projection, and thus the Gaussian band in this projection of the spectrum reflects the individual resonance. Detailed analysis of the F1 projection and the slices in the F1 direction evidence the presence of two resonances in the spectrum. The strong (R-I) and weak (R-II) (ca. 25% of the intensity) resonances exhibit the isotropic shift of 60.0 ppm (F1 = 60.4 and F2 = 59.3) and 59.2 ppm (F1 = 60.0 and F2 = 57.9), respectively.

4. Computational Models and Methods

4.1. Computational Model. A bare zeolite framework model that includes neither cations nor water molecules, proven useful in our previous studies,[25−28] is adopted to calculate the local structure around the SiO_4 and AlO_4^- tetrahedra and to predict the ^{29}Si and ^{27}Al NMR shieldings. The starting structure was generated from the X-ray structure of chabazite.[30]

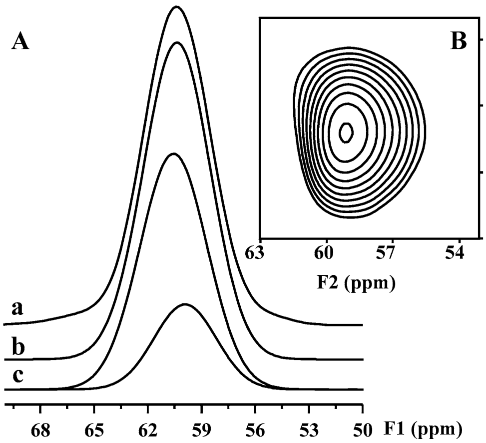

Figure 2. Analysis of the F1 projection of the ^{27}Al 3Q MAS NMR spectrum of the silicon-rich chabasite (A). Experimental spectrum (a), spectrum simulation (b), and individual Gaussian bands of the spectra simulation (c). 2D plot of the ^{27}Al 3Q MAS NMR sheared spectrum of the silicon-rich chabasite (B).

Our previous study[25,26] of ZSM-5 structures containing one Al atom per unit cell resulted in 24 distinguishable structures corresponding to Al substitution into the 24 T sites of monoclinic ZSM-5. The corresponding 24 calculated NMR shieldings were converted into ^{27}Al isotropic chemical shifts, employing the relationship between the observed resonance R-I of the silicon-rich chabazite (see Section 3) and the corresponding calculated GIAO NMR shielding (see Section 5.1).[25,26] The 24 GIAO ^{27}Al isotropic chemical shifts of ZSM were in very good agreement with the corresponding experimental values.[25,26]

4.2. QM-Pot Method and Programs Used. The QM-Pot method employed[35,36] partitions the whole system (S) into two parts. The inner part (I) is treated by QM, and the outer part (O) as well as all of the interactions between the inner and the outer layers is treated by parametrized Pot. The dangling bonds of the inner part are saturated by link hydrogen atoms. The atoms of the inner part together with the link atoms form the cluster (C). The QM-Pot approach is discussed in detail elsewhere.[37]

The calculations were performed by the QMPOT program[36] which utilizes the Turbomole program[38−42] for the QM part and the GULP program[43,44] for the periodic potential function calculations. The pure DFT method, employing the BLYP[45−47] functional and the TZVP basis set of Ahlrichs et al.,[48] was used for the QM calculations. Shell-model ion-pair potentials[49] parametrized on DFT results for zeolites[50] were employed as Pot. The electrostatic energy was evaluated by standard Ewald

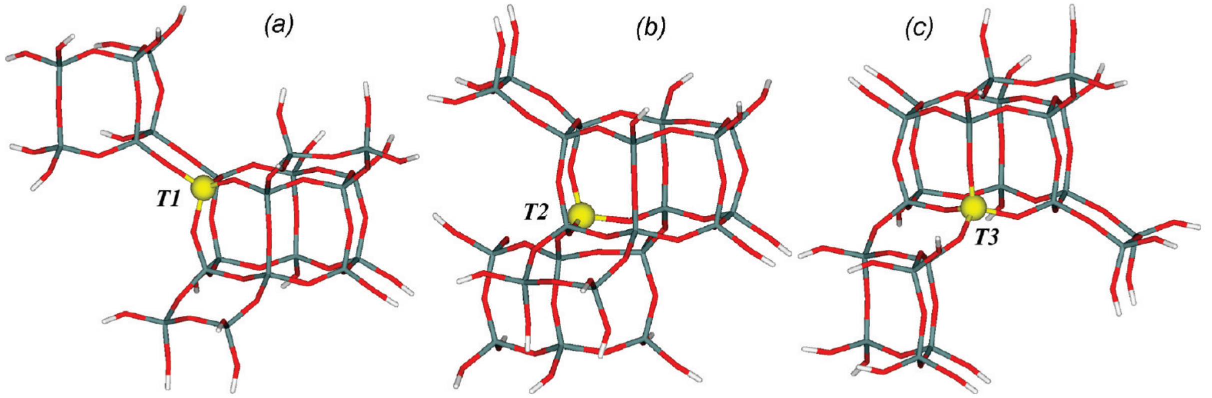

Figure 3. Five coordination shell clusters (*Si*−O−Si−O−Si−O−H_{link} and *Al*−O−Si−O−Si−O−H_{link}) having in the center the *Si* or *Al* atom located in the T1 (a), T2 (b), or T3 (c) sites. The T atom (*Si* or *Al*) is in yellow and displayed as a ball; silicon atoms are in gray, oxygen atoms in red, and link hydrogen atoms in white.

summation techniques for all cores and shells. A cutoff radius of 10 Å was chosen for the summation of short-range interactions.

4.3. Optimization of Structures. Both the lattice constants and the atomic positions of the all-silica CHA structure were optimized by the GULP program at constant pressure. Then, the silicon atom in the site of interest was replaced by an aluminum atom, and the structure and the lattice constants were further optimized at constant pressure. The optimized structures were subsequently used for defining a cluster around the Al and/or Si atoms for our QM-Pot calculations. The clusters were embedded, and the structure of the entire system was optimized by QMPOT at constant volume.

To model the effect of the presence of a silanol “nest” (a vacant T site after a dealumination) on the ^{27}Al isotropic and ^{29}Si chemical shift, the Al atom in the site of interest was removed, and the dangling bonds of the four O atoms were terminated by hydrogen atoms. The lattice parameters and atom positions were optimized by GULP at constant pressure employing Pot. The optimized structure was then utilized to prepare a cluster around both the Al or the Si atoms and the hole (removed Al atom). The clusters were then optimized at QMPOT at constant volume.

4.4. Cluster Models. To calculate the structure of SiO_4 and AlO_4^- tetrahedra of a single Si and Al atom in the framework of CHA, respectively, clusters having the Si and Al atoms in the center and including five coordination shells (Si−O−Si−O−Si−O−H_{link} and Al−O−Si−O−Si−O−H_{link}) were used, respectively (Figure 3).[19,25−28] Because of the presence of silicate rings in the framework of CHA, the created clusters contained pairs of very close H_{link} atoms. Since the close H_{link} atoms represented the same Si atom, they were replaced by the corresponding $Si(OH_{link})_2$ moiety. This was repeated until the cluster contained no such pairs.

Two types of models were employed to evaluate the effect of an Al/Si substitution on the ^{29}Si chemical shift and the SiO_4 local geometry of the nearest (Al−O−*Si*) and next-nearest (Al−O−Si−O−*Si*) silicon atoms.

The first type used a cluster centered in the *Si* atom of interest and included the Al atom as nearest (*Si*−O−Al−O−Si−O−H_{link}) and next-nearest (*Si*−O−Si−O−Al−O−H_{link}) atoms. The second utilized Al−O−*Si* and Al−O−Si−O−*Si* chains. The clusters were prepared by merging two five-coordination shell clusters (Al−O−*Si*−O−Si−O−H_{link} and *Si*−O−Al−O−Si−O−H_{link} for Al−O−*Si*; Al−O−Si−O−*Si*−O−H_{link} and *Si*−O−Si−O−Al−O−H_{link} for Al−O−Si−O−*Si*), which were centered around the Al and *Si* atoms (Figure 4). The calculations were carried out for two and four variants of the cluster for each Al−O−*Si* and Al−O−Si−O−*Si* sequence, respectively (Figure 5). The first variant contains both the Al and the *Si* atoms (Al−O−*Si* or Al−O−Si−O−*Si*), and in the second variant the Al atom is replaced by Si (Si−O−*Si* or Si−O−Si−O−*Si*). For Al−O−Si−O−*Si* chains, the third and fourth variants feature Al−O−Si−O−*Al* and Si−O−Si−O−*Al*, respectively, allowing a comparison between the effects of Al as a next-nearest neighbor on *Si* (in Al−O−Si−O−*Si*) and *Al* atoms (in Al−O−Si−O−*Al*).

The advantage of the second type with respect to the first one is that it allows evaluating the effect of the Al/Si substitution using the clusters of the same size and shape.

Clusters containing Si−$OH_{(silanol“nest”)}$ as well as Si−O−Si−$OH_{(silanol“nest”)}$ and Al−O−Si−$OH_{(silanol“nest”)}$ sequences were employed to investigate the effect of a silanol “nest” as a nearest (H−O−*Si*) and next-nearest (H−O−Si−O−*Si* and H−O−Si−O−*Al*) neighbor on the *Si*O_4 and *Al*O_4^- local geometries as well as the ^{29}Si chemical and ^{27}Al isotropic chemical shift. The clusters (Figure 6) were prepared by merging two five-coordination shell clusters which were centered around the T atom and the hole (removed atom). The effect of the presence of a silanol “nest” as a nearest neighbor on AlO_4^- was not calculated since Al−O−Al sequences are not observed in zeolite frameworks.[29] The results of our calculations of the silanol “nest” containing sequences were compared with the outcome obtained for T−O−*Si* and T−O−Si−O−*T* chains in the way as follows: H−O−*Si* with Si−O−*Si* and Al−O−*Si* (Figure 7), H−O−Si−O−*Si* with Si−O−Si−O−*Si* and Al−O−Si−O−*Si* (Figure 8), and H−O−Si−O−*Al* with Si−O−Si−O−*Al* and Al−O−Si−O−*Al* (Figure 8).

We also studied the effect of the presence of an Al(1) atom as a nearest neighbor (Al(1)−O−Al(2)) on the Al(2)O_4^- local geometry as well as the ^{27}Al isotropic chemical shift of Al(2) and vice versa. Al−O−Al sequences have not been observed in zeolites;[29] however, we attempted to estimate the possible range of the ^{27}Al isotropic chemical shift of Al present in a hypothetical Al−O−Al chain. Al(1)−O−Al(2) chains were calculated by employing clusters prepared by merging two five-coordination shell clusters (Al(1)−O−Al(2)−O−Si−O−H_{link} and Al(2)−O−Al(1)−O−Si−O−H_{link}), which were centered around the Al(1) and Al(2) atoms (Figure 9). Our calculations were performed for three variants of the cluster for each sequence. The first variant contains both Al atoms (Al(1)−O−Al(2)), and the other two variants include only one Al atom in Al(1)−O−Si(2) and Si(1)−O−Al(2) chains (Figure 10).

4.5. Calculation of ^{29}Si and ^{27}Al NMR Shielding. Subsequent to the QM-Pot structure determination, the Gaussian

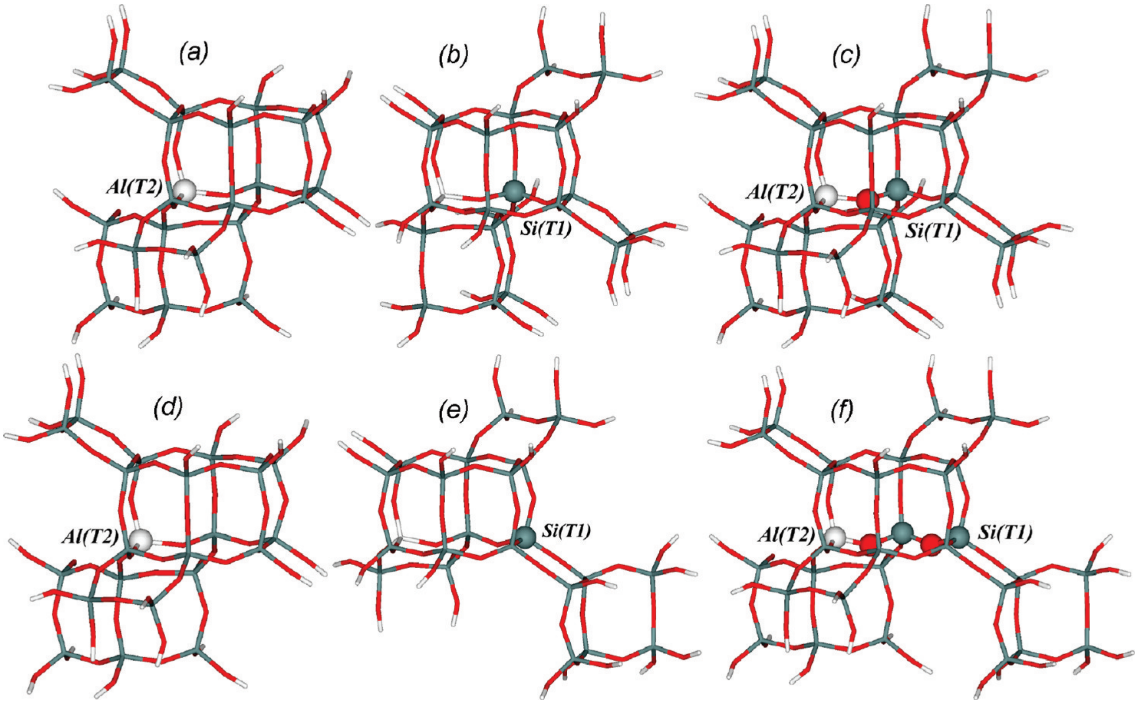

Figure 4. Clusters centered around Al(T2) for Al−O−*Si* (a), Si(T1) for Al−O−*Si* (b), Al(T2) for Al−O−Si−O−*Si* (d), and Si(T1) for Al−O−Si−O−*Si* (e). The merged clusters for Al(T2)−O−*Si*(T1) (c) and Al(T2)−O−Si−O−*Si*(T1) (f). Silicon atoms are in gray, aluminum atoms in white, oxygen atoms in red, and link hydrogen atoms in white. The atoms corresponding to the Al−O−*Si* and Al−O−Si−O−*Si* sequences are displayed as balls.

program[51] was employed to calculate NMR shielding tensors for the atoms of the optimized clusters at the BLYP/TZVP level using the GIAO method.[18] Note that a higher NMR shielding corresponds to a lower (isotropic) chemical shift.

5. Computational Results

5.1. T Sites. Our QM-Pot calculations of the CHA framework (*P*1 symmetry) containing one Al atom in a supercell composed of four unit cells of CHA (Si/Al 47) resulted in three very close but distinguishable AlO_4^- structures which slightly differ in both the AlO_4 local geometry as well as the ^{27}Al shieldings (Table 1). The relative energies of Al in the three T sites of CHA are all within 3 kcal/mol (Table 1). The Al/Si substitution also caused the single T site of all-silica chabazite[52] to split into three very close T sites having slightly different SiO_4 local geometries and ^{29}Si NMR shieldings (Table 2).

5.2. Effect of an Al/Si Substitution. We employed two types of models (see Section 4.4) to evaluate the effect of an Al/Si substitution on the ^{29}Si chemical shift and the SiO_4 local geometry of the nearest (Al−O−*Si*) and next-nearest (Al−O−Si−O−*Si*) silicon atoms. The first type used yielded a systematic downshift of the ^{29}Si chemical shift by 4.6−9.8 ppm for Al−O−*Si* (Table 3) and by 0.7−1.4 ppm for Al−O−Si−O−*Si* (Table 3). The second type utilized also gave a systematic downshift by 4.2−10.8 ppm for Al−O−*Si* (Table 4) and by 0.2−2.3 ppm for Al−O−Si−O−*Si* (Table 5). The calculated changes of the average T−O−T angle range from −0.7 to +3.8° for Al−O−*Si* (Table 4) and from −0.3 to +1.0° for Al−O−Si−O−*Si* (Table 5). The calculated effect of an Al/Si substitution on the ^{27}Al isotropic chemical shift and AlO_4^- local geometry of the next-nearest (Al−O−Si−O−*Al*) aluminum atoms is an increase from 0.2 to 2.9 ppm and from 0.0 to +2.1°, respectively (Table 5). The corresponding calculated ^{27}Al and ^{29}Si shieldings, ^{29}Si chemical shifts, and average T−O−T angles of SiO_4 and AlO_4^- tetrahedra are listed in Tables 3, 4, and 5.

5.3. Effect of a Silanol "Nest". Our QMPOT results reveal a systematic and significant downshift of the ^{29}Si chemical shift by 10.7−16.4 ppm (Table 4) caused by the presence of a silanol "nest" as a nearest (H−O−*Si*) neighbor, while the corresponding effect of a silanol "nest" in H−O−Si−O−*Si* is a small systematic downshift up to 1.3 ppm (Table 5). Our results also indicate that there is no systematic effect of a silanol "nest" as a next-nearest neighbor (H−O−Si−O−*Al*) on the ^{27}Al isotropic chemical shift, as its values are smaller for some *Al* atoms (up to −3.6 ppm) atoms and greater for others (up to +2.9 ppm) (Table 5). The calculated changes of the average T−O−T angle range from 7.5 to 11.5° for H−O−*Si* (Table 4), from −0.3 to +0.9° for H−O−Si−O−*Si*, and from −1.8 to +2.4° for H−O−Si−O−*Al* (Table 5).

5.4. Al−O−Al Sequences. Our calculations show (Table 6) that the presence of Al in a hypothetical Al−O−Al chain would lead to ^{27}Al isotropic chemical shifts and average T−O−T angles which would be systematically larger by 6.9−9.3 ppm and by −0.3 to 3.3°, respectively, than those obtained for a single Al atom in the chabazite framework.

5.5. Correlation between the ^{29}Si Chemical Shift and the Average T−O−T Angle. A simple linear correlation between the ^{29}Si chemical shift δ(Si) and the average T−O−T angle (θ) of the zeolite framework was established for zeolites with a high Si/Al ratio by Thomas.[9,10]

$$\delta(\mathrm{Si}) = -25.44 - 0.5793\theta \text{ ppm}$$

The calculated GIAO ^{29}Si NMR shielding values are plotted against the average T−O−T angles for Al−O−*Si* (Table 4) and Al−O−Si−O−*Si* sequences (Table 5) in Figures 11 and 12, respectively. Figure 11 reveals an excellent correlation for Al−O−*Si* sequences, while Figure 12 shows that the relationship between the ^{29}Si chemical shift and the local geometry of SiO_4

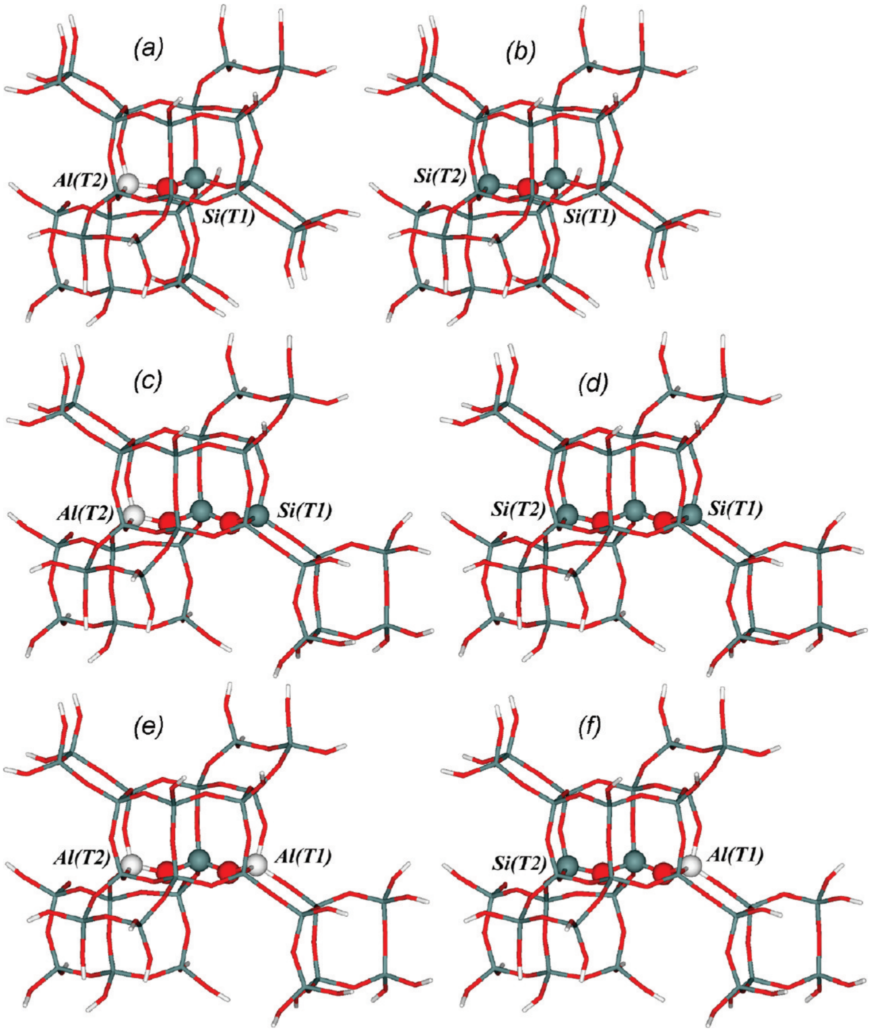

Figure 5. Two (a and b) and four (c, d, e, and f) variants of the cluster for the Al−O−*Si* and Al−O−Si−O−*Si* sequences, respectively. The first variant contains both *Al* and *Si* atoms (Al−O−*Si* (a) and Al−O−Si−O−*Si* (c)). In the second variant the Al is replaced by Si (Si−O−*Si* (b) and Si−O−Si−O−*Si* (d)). For Al−O−Si−O−*Si* chains, the third and fourth variants feature Al−O−Si−O−*Al* (e) and Si−O−Si−O−*Al* (f), respectively, allowing a comparison between the effects of Al as a next-nearest neighbor on *Si* (in Al−O−Si−O−*Si*) and *Al* atoms (in Al−O−Si−O−*Al*). Silicon atoms are in gray, aluminum atoms in white, oxygen atoms in red, and link hydrogen atoms in white. The atoms corresponding to the Al−O−*Si* and Al−O−Si−O−*Si* sequences are displayed as balls.

tetrahedron for Al−O−Si−O−*Si* sequences is more complex than a simple linear correlation between the shift and the average T−O−T angle.

5.6. Correlation between the ^{27}Al Isotropic Chemical Shift and the Average T−O−T Angle. On the basis of a comparison between the crystallographic and the ^{27}Al NMR data of aluminum-rich zeolites, Lippmaa et al.[11] suggested a linear correlation between the ^{27}Al NMR isotropic chemical shift δ(Al) and the average T−O−T angle (θ) of the zeolite framework.

$$\delta(\mathrm{Al}) = -0.50\theta + 132\ \mathrm{ppm}$$

The calculated GIAO ^{27}Al NMR shielding values are plotted against the average T−O−T angles for Al−O−Si−O−*Al* sequences (Table 5) in Figure 13. The corresponding plot shows that the linear correlation does not hold at all for Al−O−Si−O−*Al* sequences in the framework of the silicon-rich chabazite. This conclusion regarding the failure of the linear correlation is in agreement with that reached previously for ZSM-5.[26,27]

6. Discussion

6.1. ^{27}Al Isotropic Chemical Shift of the Isolated AlO_4^- Tetrahedra. An Al/Si substitution breaks down the symmetry of the chabazite framework, and one distinguishable T site splits into three T sites having slightly different local geometries (Table 1). The splitting of one T site is reflected in three ^{27}Al NMR shielding values; however, two of them are very similar (Table 1). This result is in agreement with the two observed ^{27}Al NMR resonances for the silicon-rich chabazite (Table 1). The differences of the local structures as well as the ^{27}Al NMR shielding values between the T1 and the T3 sites of CHA are an order of magnitude smaller than the corresponding differences between the T20 (smallest ^{27}Al isotropic chemical shift) and the T24 (largest ^{27}Al isotropic chemical shift) sites of the ZSM-5 zeolite.[25,26] Since there is no assignment problem for CHA, the calculated ^{27}Al NMR shielding of 490.0 ppm and the measured ^{27}Al isotropic chemical shift of 60.0 ppm can be used as a secondary internal standard to convert the calculated ^{27}Al NMR shieldings into ^{27}Al isotropic chemical shifts.[25,26]

6.2. ^{29}Si Chemical Shift of SiO_4 Tetrahedra. The observed ^{29}Si NMR spectrum of the silicon-rich chabazite (Figure 1) reveals three resonances: one strong and two weak and broad.

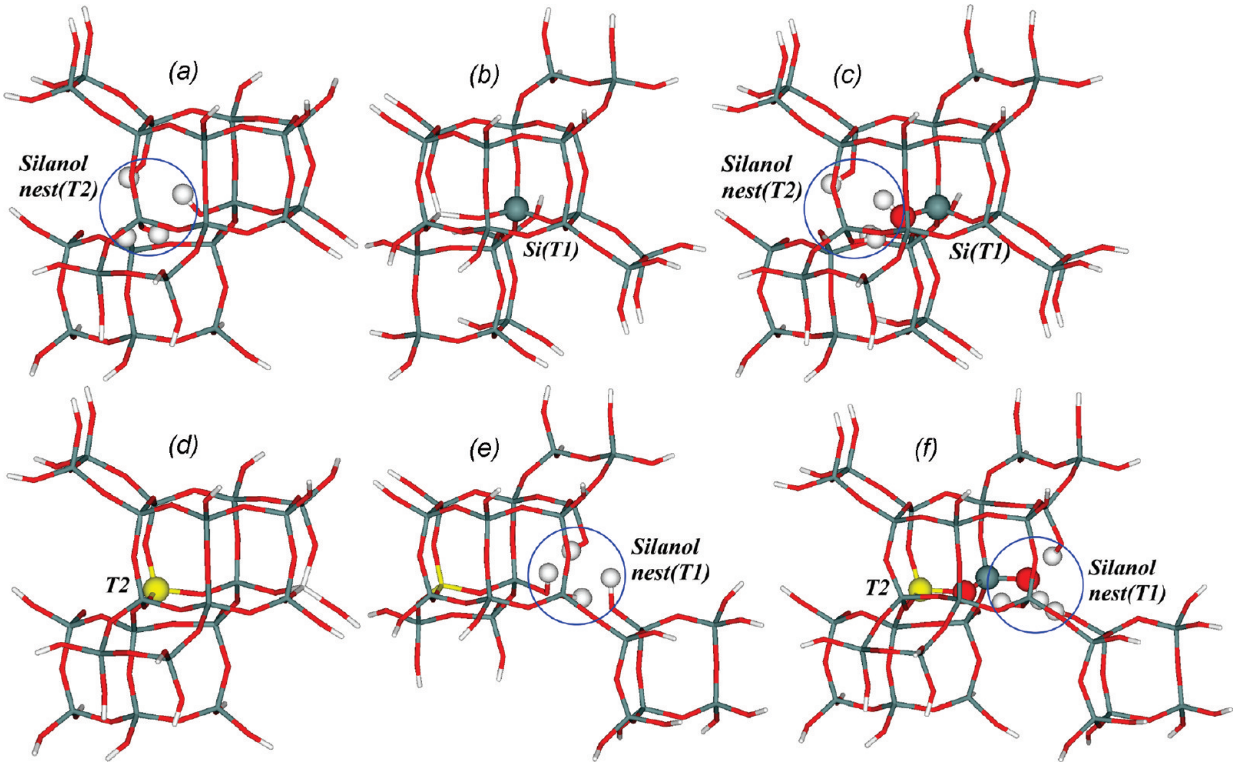

Figure 6. Clusters centered around the hole (missing Al) for H−O−*Si* (a) and H−O−Si−O−*T* (*T* = *Si* or *Al*) (e), Si(T1) for H−O−*Si* (b), and T(T2) for H−O−Si−O−*T* (*T* = *Si* or *Al*) (d). The merged clusters for H−O−*Si* (c) and for H−O−Si−O−*T* (*T* = *Si* or *Al*) (f). Silicon atoms are in gray, oxygen atoms in red, and hydrogen atoms in white, and the *T* atom is in yellow. The atoms corresponding to the H−O−*Si* and H−O−Si−O−*T* sequences are displayed as balls.

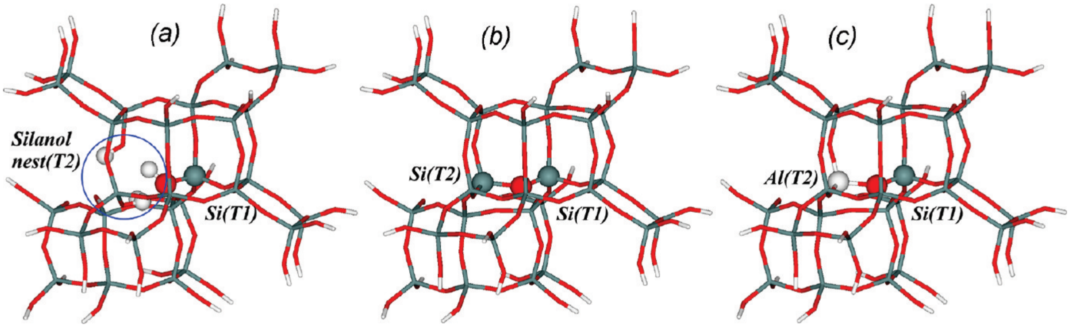

Figure 7. H−O−*Si* (a), Si−O−*Si* (b), and Al−O−*Si* (c) sequences. Silicon atoms are in gray, aluminum atom in white, oxygen atoms in red, and hydrogen atoms in white. The atoms corresponding to the sequences are displayed as balls.

The strong band at −111.5 ppm corresponds to the Si(4Si) site and is very close to that at −111.4 ppm obtained for the all-silica chabazite.[52] The two observed weak resonances at −110.8 and −110.3 ppm correspond to *Si* atoms in Al−O−Si−O−*Si* and H−O−Si−O−*Si* sequences (Sections 6.4 and 6.6). Our calculations of the ^{29}Si NMR shielding values of Si atoms of the chabazite (Si/Al 47) yielded 450.2 and 450.3 ppm for two and one distinguishable T sites (Table 2), respectively, indicating that one ^{29}Si NMR resonance of all-silica chabazite[52] splits into three very close resonances. However, the splitting is not observed since it is beyond the detection limit of a ^{29}Si MAS NMR experiment on an Al containing zeolite because of the perturbing effects of the framework Al atoms on the local geometry of SiO_4 tetrahedra and thus on the width of the ^{29}Si resonances.[53] We relate the calculated shielding value of 450.2 ppm to the experimental chemical shift value of −111.5 ppm, which allows a conversion of the calculated ^{29}Si NMR shieldings into ^{29}Si chemical shifts.

The two weak resonances at −105.7 and −104.5 ppm can be assigned to Si(3Si,1Al)[12,54,55] and the three weak resonances of −102.0, −101.0, and −99.9 ppm to SiOH.[12,54,55] The latter assignment is confirmed by a CP experiment (Figure 1). Furthermore, the band at −102.0 ppm is close to that at −101.4 ppm which was assigned to SiOH for the all-silica chabazite.[52]

6.3. Effect of Al on *Si* in Al−O−*Si*. It is well known that Al as the nearest neighbor strongly influences the Si chemical shift. The Si(3Si,1Al) signal is downshifted by some 6 ppm for the faujasite zeolite having one framework T site. Similar values of the downshift were reported for silicon-rich zeolites.[12,54,55] However, the downshift can be larger, reaching 9 ppm for the silicon-rich zeolite of the β structure,[56] and it might reach even somewhat larger values.[13] Our computational results are in agreement with these experimental observations. Our calculations show a change of the local geometries of SiO_4: the average T−O−T angle changed by up to a few degrees (Table 4) as well as a systematic downshift of the ^{29}Si chemical shifts by 4.6−9.8 ppm (first type of models; Table 3) and 4.2−10.8 ppm (second type of models; Table 4).

Significant differences between ^{29}Si chemical shifts of Si atoms with different Al neighbors open a possibility to employ

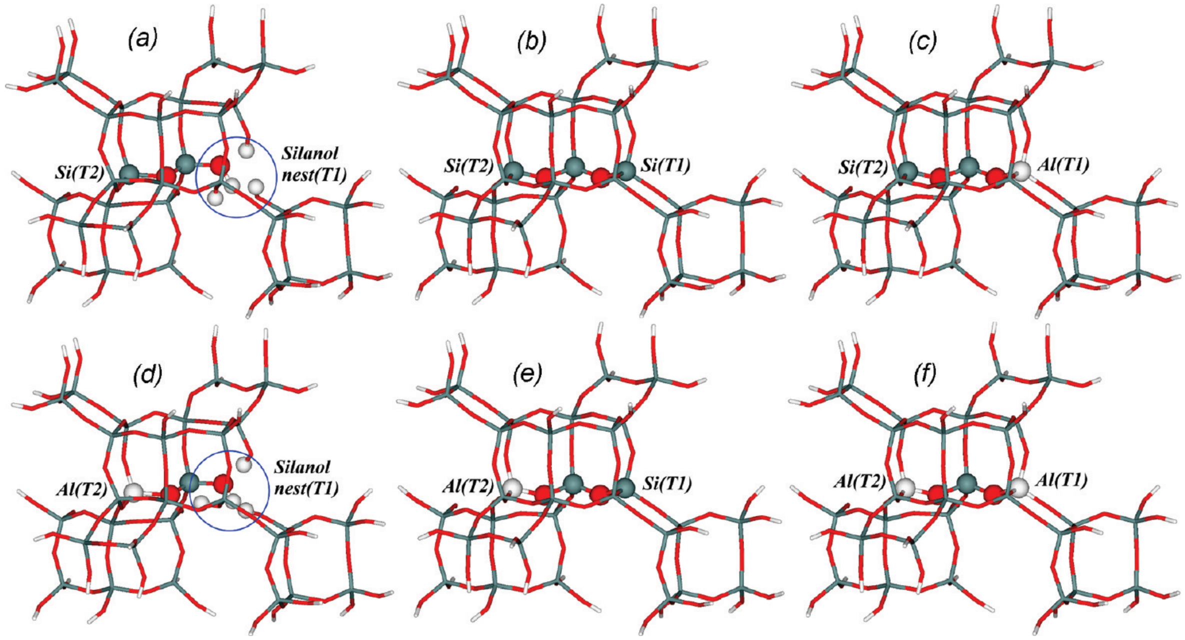

Figure 8. H−O−Si−O−*Si* (a), Si−O−Si−O−*Si* (b), Al−O−Si−O−*Si* (c), H−O−Si−O−*Al* (d), Si−O−Si−O−*Al* (e), and Al−O−Si−O−*Al* (f) sequences. Silicon atoms are in gray, aluminum atoms in white, oxygen atoms in red, and hydrogen atoms in white. The atoms corresponding to the sequences are displayed as balls.

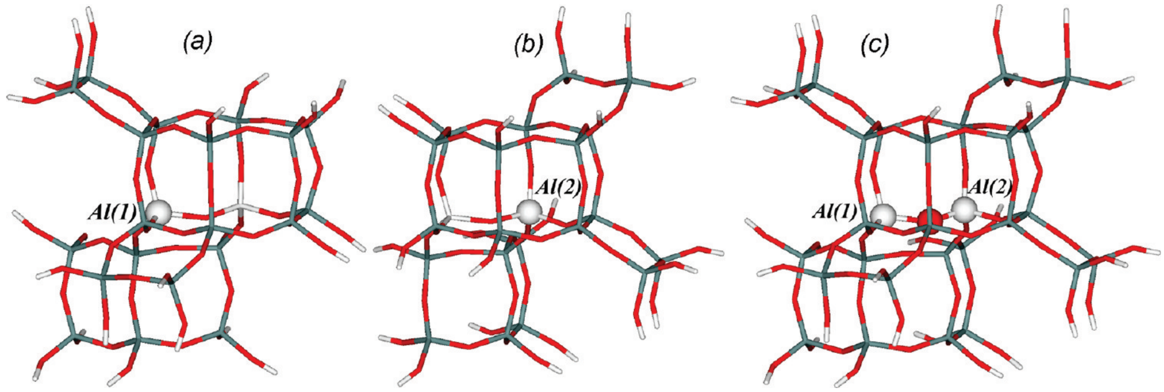

Figure 9. Clusters centered around Al(1) (a) and Al(2) (b). The merged cluster for Al(1)−O−Al(2) (c). Silicon atoms are in gray, aluminum atoms in white, oxygen atoms in red, and link hydrogen atoms in white. The atoms corresponding to the Al(1)−O−Al(2) sequences are displayed as balls.

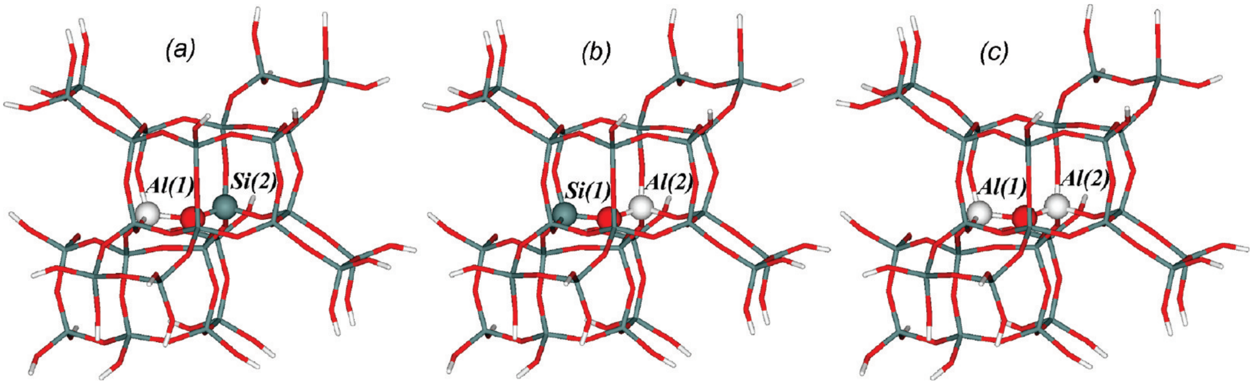

Figure 10. Three variants of the cluster for the Al(1)−O−Al(2) sequences. The first (a) and second (b) variants contain only one Al. The third variant features both Al atoms (Al(1) and Al(2)). Silicon atoms are in gray, aluminum atoms in white, oxygen atoms in red, and link hydrogen atoms in white. The atoms corresponding to the Al(1)−O−Al(2) sequences are displayed as balls.

^{29}Si MAS NMR spectroscopy to identify the Al site in silicon-rich zeolites with a low number of distinguishable framework T sites, that is, a low number of different Si−O−Al sequences. It is noteworthy that our QM-Pot predictions indicate that the change of the ^{29}Si chemical shift of Si(3Si,1Al) can reach large values (up to about 10−11 ppm). QM-Pot calculations employing the bare framework model allow more detailed interpretations of complex ^{29}Si MAS NMR spectra of silicon-rich zeolites

TABLE 1: ^{27}Al NMR Shieldings (ppm), Average T−O−T Angles (deg), QM-Pot Relative Energies (kcal/mol), and Observed ^{27}Al Isotropic Chemical Shifts (ppm) of Al in the Three T Sites of Chabazite

T site	shielding	T−O−T	energy	$^{27\text{Al}}\delta^{\text{OBSERVED}}$
T1[a]	490.4	145.4	0.0	59.2
T2	490.0	145.6	1.6	60.0
T3	489.9	144.7	3.4	60.0

[a] The Cartesian coordinates with T site designations are shown in the Supporting Information.

TABLE 2: ^{29}Si NMR Shieldings (ppm), Average T−O−T Angles (deg), and Observed ^{29}Si Chemical Shifts (ppm) of Si in the Three T Sites of Chabazite

T site	shielding	T−O−T	$^{29\text{Si}}\delta^{\text{OBSERVED}}$
T1	450.3	147.9	−111.5
T2	450.2	147.8	−111.5
T3	450.2	147.8	−111.5

with more distinguishable T sites and thus provide a complementary tool to ^{27}Al MQ MAS NMR spectroscopy to study the Al distribution in silicon-rich zeolites.

6.4. Effect of Al on *Si* in Al−O−Si−O−*Si* and *Al* in Al−O−Si−O−*Al*. In contrast to the knowledge of the effect of Al atoms as a nearest neighbor (Al−O−*Si*) on the ^{29}Si chemical shift, there is only very limited knowledge of the corresponding influence of Al as a next-nearest neighbor (Al−O−Si−O−*Si*) on the ^{29}Si chemical shift.[5] The effect of Al as a next-nearest neighbor on the ^{27}Al isotropic chemical shift in the ZSM-5 framework was investigated in our prior study.[27] Our calculations revealed that the ^{27}Al NMR isotropic chemical shift of Al framework atoms in ZSM-5 can be significantly affected (a decrease of the ^{27}Al isotropic chemical shift of Al up to 2 ppm for some Al−O−Si−O−Al sequences and an increase up to 4 ppm for the others) by the presence of an Al atom as a next-nearest neighbor because of changes of the local geometry of AlO_4^- tetrahedra (a decrease of the average Al−O−Si angle of AlO_4^- up to 8° for some Al−O−Si−O−Al sequences and an increase up to 6° for the others). Our calculations showed that there is no systematic contribution of Al in Al−O−Si−O−Al chains to the ^{27}Al isotropic chemical shift, and not even the direction can be predicted without calculating the sequence.[27]

Our calculations of the influence of Al atoms as a next-nearest neighbor (Al−O−Si−O−*Si*) on the ^{29}Si chemical shift of *Si* show only a small effect on the local geometry of *Si*O$_4$ tetrahedra. The calculated downshift ranges from 0.2 to 2.3 ppm, and the change of the average T−O−T angles is up to a degree (Table 5). The calculated effect of Al atoms as a next-nearest neighbor (Al−O−Si−O−*Al*) on the ^{27}Al chemical shift of *Al* is similar to that on *Si*. The ^{27}Al isotropic chemical shifts of *Al* are systematically larger by 0.2−2.9 ppm, and the average T−O−T angles change up to 2°.

It is noteworthy that the effect of Al atoms as a next-nearest neighbor (Al−O−Si−O−*Al*) on the ^{27}Al isotropic chemical shift of *Al* is less pronounced in the chabazite zeolite than in ZSM-5. Furthermore, the presence of Al in Al−O−Si−O−*Al* in CHA makes a similar systematic contribution to ^{27}Al isotropic chemical shifts as the presence of Al in Al−O−Si−O−*Si* to ^{29}Si chemical shifts. The effect of Al as a next-nearest neighbor is different for Al−O−Si−O−*Al* sequences in the CHA and ZSM-5 frameworks. This difference might reflect a different rigidity of the CHA framework with respect to the ZSM-5 framework and indicates that the effect of Al atoms as a next-nearest neighbor (Al−O−Si−O−*Al*) on the ^{27}Al isotropic chemical shift of *Al* is zeolite-framework dependent and can be obtained only from calculations of Al−O−Si−O−*Al* sequences in the zeolite framework of interest.

The previously described long-range effect of the framework perturbation by an Al/Si substitution can explain the effect of the presence of Al in the framework on the width and shape of ^{29}Si NMR resonances in zeolites.[53] In contrast to a narrow Lorentz shaped curve of ^{29}Si resonance, corresponding to one well-defined arrangement of a Si crystallographic site in a pure all-silica material, a Gaussian shaped broad resonance of ^{29}Si in Al-containing materials represents an envelope of a number of resonances corresponding to Si atoms in the same crystallographic site but with local arrangements changed because of the presence of Al as a neighbor in Al−O−(Si−O)$_n$−Si chains ($n = 1 \rightarrow \infty$). Note that, in contrast to the long-range structural effects of an Al/Si substitution on the SiO_4 local geometry, the heteronuclear interaction between ^{27}Al and ^{29}Si represents a rather short-range effect that explains neither the broadening of ^{29}Si resonances in high-silica zeolites (Si/Al > 100) nor the effect of only traces of Al atoms in all-silica zeolites.[53] Similar long-range effects of Al atoms as a neighbor on the local geometry of AlO_4^- tetrahedra can be inferred. An analogy with the above-described effect of Al on the ^{29}Si MAS NMR spectra explains the fact that the quadrupolar interaction is not a key parameter responsible for the broadening of ^{27}Al resonances in MAS NMR and MQ MAS NMR experiments on silicon-rich zeolites. Note that the same widths of ^{27}Al NMR resonances were observed for F1 and F2 projections of the ^{27}Al MQ MAS NMR spectra both for the ZSM-5[25−27] and the β zeolite.[57]

6.5. Effect of Silanols on *Si* in H−O−*Si*. Terminal silanol groups as well as silanol "nests" are important defects in zeolite frameworks. A silanol "nest" is a model of a defect (vacant T site after a dealumination) in a zeolite framework. We studied their influence as nearest neighbors on the local geometry of SiO_4 and ^{29}Si chemical shift. Our calculations reveal systematically smaller average T−O−T angles (by 7.5−11.5°) for SiO_4 and a systematic downshift of the Si(3Si,OH) chemical shift by 10.7−16.4 ppm (Table 4). This range is still in agreement with the observed range of 9.5−11.6 ppm (Figure 1) which corresponds to terminal silanol groups on the outer surface of the zeolite crystals rather than to vacant T sites (silanol "nests") in the zeolite framework. Since a significant difference between the ^{29}Si chemical shifts of Si(3Si,OH) corresponding to terminal silanols (our ^{29}Si NMR experiment) and to the silanol nests formed in a dealuminated zeolite framework (our calculations) was not found, we can assume that the OH groups in silanol nests represent a suitable model to describe Si−OH groups in silicon-rich zeolites. Note that, to the best of our knowledge, varying ^{29}Si chemical shifts have not been reported for silanol nests in partially dealuminated zeolites and terminal silanols in ideal zeolite structures. Our calculations are in agreement with previous experimental findings[7,58−61] that there is an overlap of the ^{29}Si chemical shift of Si(3Si,1Al) and Si(3Si,OH), confirming that a combination of a single pulse and CP ^{29}Si NMR experiment is essential to interpret results of ^{29}Si MAS NMR experiments. This indicates that the uncertainty of the interpretation and quantitative evaluation of the ^{29}Si MAS NMR spectra of mordenite samples[62] is not a specific property of the mordenite structure and might be (at least for some specific T sites) a general problem of silicon-rich zeolite matrices. Table 4 allows comparison of the effect of a silanol group (OH) with the influence of the corresponding Al/Si substitution on the ^{29}Si chemical shift of the nearest silicons. Both effects are systematic

TABLE 3: ^{29}Si NMR Shieldings (ppm) and Chemical Shifts (ppm) for *Si* of the Al−O−*Si* and Al−O−Si−O−*Si* Sequences

sequence	shielding	Δ[a,b]	^{29}Siδ[c]	sequence	shielding	Δ[a,b]	^{29}Siδ[c]
Al(T2)−O−*Si*(*T1*)[d]	445.6	4.6	−106.9	Al(T3)−O−*Si*(*T1*)	442.3	7.9	−103.6
Al(T2)−O−*Si*(*T3*)	443.3	6.9	−104.6	Al(T3)−O−*Si*(*T3*)[e]	444.5	5.7	−105.8
Al(T2)−O−*Si*(*T1*)[d]	441.9	8.3	−103.2	Al(T1)−O−*Si*(*T2*)[f]	445.6	4.6	−106.9
Al(T2)−O−*Si*(*T2*)	441.7	8.5	−103.0	Al(T1)−O−*Si*(*T3*)	440.4	9.8	−101.7
Al(T3)−O−*Si*(*T3*)[e]	441.8	8.4	−103.1	Al(T1)−O−*Si*(*T1*)	443.8	6.4	−105.1
Al(T3)−O−*Si*(*T2*)	441.8	8.4	−103.1	Al(T1)−O−*Si*(*T2*)[f]	441.5	8.7	−102.8
Al(T2)−O−Si(T3)−O−*Si*(*T3*)	449.5	0.7	−110.8	Al(T3)−O−Si(T3)−O−*Si*(*T3*)	449.2	1.0	−110.5
Al(T1)−O−Si(T3)−O−*Si*(*T3*)	448.8	1.4	−110.1				

[a] The difference between ^{29}Si NMR shielding values of *Si* and Si having no nearest or next-nearest Al neighbor (450.2 ppm). [b] A positive value indicates a downshift of the corresponding ^{29}Si chemical shift of the *Si* atom present in the Al−O−*Si* sequences with respect to the ^{29}Si chemical shift of the Si atom having no nearest or next-nearest Al neighbor. [c] The ^{29}Si chemical shifts were obtained by a conversion of the GIAO shieldings using the calculated and measured shielding/shift values of 450.2 ppm and −111.5 ppm, respectively, for the chabazite sample. $^{29\text{Si}}\delta = -111.5 + \Delta(\text{shieldings})$. [d–f] These two sequences have symmetrically inequivalent oxygen atoms.

TABLE 4: ^{29}Si NMR Shieldings (ppm) and Chemical Shifts (ppm) and Average T−O−T Angles (deg) for *Si* of X−O−*Si* (X = H, Al, and Si) Sequences

sequence	shielding	Δ[a]	^{29}Siδ[b]	T−O−T	Δ
Al(T2)−O−*Si*(*T2*)	439.6	10.8	−100.7	144.2	3.8
Si(T2)−O−*Si*(*T2*)	450.4			148.0	
H(T2)−O−*Si*(*T2*)	439.7	10.7	−100.8	140.5	7.5
Al(T2)−O−*Si*(*T3*)	445.1	5.5	−106.0	147.6	0.6
Si(T2)−O−*Si*(*T3*)	450.6			148.2	
H(T2)−O−*Si*(*T3*)	436.5	14.1	−97.4	138.3	9.9
Al(T2)−O−*Si*(*T1*)[c]	446.4	4.2	−107.3	148.6	−0.7
Si(T2)−O−*Si*(*T1*)	450.6			147.9	
H(T2)−O−*Si*(*T1*)	436.9	13.7	−97.8	139.5	8.4
Al(T2)−O−*Si*(*T1*)[c]	440.5	9.6	−101.9	144.8	2.8
Si(T2)−O−*Si*(*T1*)	450.1			147.6	
H(T2)−O−*Si*(*T1*)	433.7	16.4	−95.1	136.1	11.5
Al(T3)−O−*Si*(*T3*)[d]	440.8	9.2	−102.3	144.7	2.9
Si(T3)−O−*Si*(*T3*)	450.0			147.6	
H(T3)−O−*Si*(*T3*)	434.5	15.5	−96.0	137.4	10.2
Al(T3)−O−*Si*(*T3*)[d]	446.5	4.2	−107.3	148.7	−0.7
Si(T3)−O−*Si*(*T3*)	450.7			148.0	
H(T3)−O−*Si*(*T3*)	436.5	14.2	−97.3	138.8	9.2
Al(T3)−O−*Si*(*T2*)	445.4	5.1	−106.4	147.8	0.4
Si(T3)−O−*Si*(*T2*)	450.5			148.2	
H(T3)−O−*Si*(*T2*)	436.0	14.5	−97.0	140.3	7.9
Al(T3)−O−*Si*(*T1*)	442.4	7.8	−103.7	146.2	2.0
Si(T3)−O−*Si*(*T1*)	450.2			148.2	
H(T3)−O−*Si*(*T1*)	439.0	11.2	−100.3	139.5	8.7
Al(T1)−O−*Si*(*T2*)[e]	446.1	4.4	−107.1	148.4	−0.6
Si(T1)−O−*Si*(*T2*)	450.5			147.8	
H(T1)−O−*Si*(*T2*)	436.8	13.7	−97.8	139.0	8.8
Al(T1)−O−*Si*(*T2*)[e]	441.2	8.8	−102.7	145.0	2.6
Si(T1)−O−*Si*(*T2*)	450.0			147.6	
H(T1)−O−*Si*(*T2*)	434.4	15.6	−95.9	137.3	10.3
Al(T1)−O−*Si*(*T3*)	442.4	7.9	−103.6	146.4	1.6
Si(T1)−O−*Si*(*T3*)	450.3			148.0	
H(T1)−O−*Si*(*T3*)	435.2	15.1	−96.4	137.9	10.1
Al(T1)−O−*Si*(*T1*)	444.6	6.0	−105.5	147.5	0.7
Si(T1)−O−*Si*(*T1*)	450.6			148.2	
H(T1)−O−*Si*(*T1*)	436.6	14.0	−97.5	138.5	9.7

[a] A positive value indicates a downshift of the corresponding ^{29}Si chemical shift of the *Si* atom present in the Al−O−*Si* or H−O−*Si* sequences with respect to the ^{29}Si chemical shift of *Si* in Si−O−*Si*. [b] The ^{29}Si chemical shifts were obtained by a conversion of the GIAO shieldings using the calculated and measured shielding/shift values of 450.2 ppm and −111.5 ppm, respectively, for the chabazite sample. $^{29\text{Si}}\delta = -111.5 + \Delta(\text{shieldings})$. [c–e] These two sequences have symmetrically inequivalent oxygen atoms.

downshifts of the chemical shifts of Si(3Si,OH) and Si(3Si,1Al); however, the former is significantly larger, by up to 10 ppm, than the latter. Al in AlO$_4^-$ and Si in SiO$_4$ are isoelectronic, and therefore the changes of the local geometry caused by the Al/Si substitution are responsible for the downshift. On the other hand, the H atom of the silanol is not isoelectronic with the Si atom of SiO$_4$, and thus the downshift is caused by both the changes of the local geometry as well as an electronic effect. This explains why the perturbation of the SiO$_4$ local geometry and the corresponding ^{29}Si chemical shift by a neighboring silanol (OH) is significantly larger than that caused by a neighboring Al atom.

6.6. Effect of Silanols on *Si* in H−O−Si−O−*Si* and *Al* in H−O−Si−O−*Al*.

Table 5 compares the calculated effects of a silanol group and an Al/Si substitution on the ^{29}Si chemical and ^{27}Al isotropic chemical shift of *Si* and *Al*, respectively, and the local geometries of *Si*O$_4$ and *Al*O$_4^-$ tetrahedra, respectively.

The calculated effect of a silanol group in H−O−Si−O−*Si* on the ^{29}Si chemical shifts of *Si* is a small, systematic downshift up to 1.3 ppm which is close to that caused by the presence of Al in Al−O−Si−O−*Si* (up to 2.3 ppm).

On the other hand, our computational results (Table 5) reveal that, in contrast to the effect of Al in Al−O−Si−O−*Al*, there is no systematic contribution of a silanol group in H−O−Si−O−*Al* to the ^{27}Al isotropic chemical shift of *Al* (changes in the range from −3.6 to +2.9 ppm). Not even the direction can be predicted without explicit DFT calculations of each chain. Also, the changes of the average T−O−T angles of AlO$_4^-$ are not systematic.

The presence of silanol groups in the framework has a similar effect on the width and shape of ^{29}Si and ^{27}Al NMR resonances in zeolites as the occurrence of Al in the zeolite matrix. Gaussian shaped broad resonances of ^{29}Si and ^{27}Al in materials containing silanol groups represent an envelope of a number of resonances corresponding to Si and Al, respectively, atoms in the same crystallographic site but with local arrangements changed because of the presence of SiOH.

6.7. Effect of Al on *Al* in Al−O−*Al*.

Al−O−Al chains are not observed in zeolite frameworks. The Loewenstein rule,[29] which forbids Al−O−Al, is based on indirect evidence, specifically, the absence of the Al−O−Al sequences in zeolite frameworks for zeolites with Si/Al = 1. This absence results from the exclusive presence of Si(4Al) species in these frameworks.[63] Another piece of indirect evidence against the presence of Al−O−Al chains in aluminosilicate frameworks is that the Si/Al ratio reaches 1:1 at best.[64] It was shown experimentally that compliance to the Loewenstein rule is kinetic in origin.[64] Moreover, the development of new methods of zeolite synthesis in various environments (e.g., using strongly acidic fluoric acid or highly specific-structure directing agents) might make possible structures having an otherwise very low probability of occurrence which can be formed in zeolite materials. It was shown that the formation of Al−O−Al chains

TABLE 5: ^{29}Si and ^{27}Al NMR Shieldings (ppm), ^{29}Si Chemical Shifts (ppm), and Average T−O−T Angles (deg) for *Si* and *Al* of Al−O−Si−O−*Si* and Al−O−Si−O−*Al* Sequences, Respectively

sequence	shielding	Δ	$^{29Si}\delta^a$	T−O−T	Δ
Al(T2)−O−Si(T3)−O−Si(T3)	449.3	0.9[b]	−110.6	147.5	0.3
Si(T2)−O−Si(T3)−O−Si(T3)	450.2			147.8	
H(T2)−O−Si(T3)−O−Si(T3)	450.1	0.1[b]	−111.4	147.8	0.0
Al(T2)−O−Si(T3)−O−Al(T3)	487.9	1.2[c]		145.4	0.0
Si(T2)−O−Si(T3)−O−Al(T3)	489.1			145.4	
H(T2)−O−Si(T3)−O−Al(T3)	489.9	−0.8[c]		145.6	−0.2
Al(T2)−O−Si(T1)−O−Si(T1)	449.9	0.5[b]	−111.0	147.7	0.3
Si(T2)−O−Si(T1)−O−Si(T1)	450.4			148.0	
H(T2)−O−Si(T1)−O−Si(T1)	449.2	1.2[b]	−110.3	147.1	0.9
Al(T2)−O−Si(T1)−O−Al(T1)	488.2	0.9[c]		144.2	0.6
Si(T2)−O−Si(T1)−O−Al(T1)	489.1			144.8	
H(T2)−O−Si(T1)−O−Al(T1)	487.5	1.6[c]		145.7	−0.9
Al(T2)−O−Si(T2)−O−Si(T3)	450.1	0.2[b]	−111.3	148.1	−0.3
Si(T2)−O−Si(T2)−O−Si(T3)	450.3			147.8	
H(T2)−O−Si(T2)−O−Si(T3)	450.2	0.1[b]	−111.4	147.7	0.1
Al(T2)−O−Si(T2)−O−Al(T3)	489.6	0.4[c]		144.8	0.7
Si(T2)−O−Si(T2)−O−Al(T3)	491.0			145.5	
H(T2)−O−Si(T2)−O−Al(T3)	491.7	−0.7[c]		145.6	−0.1
Al(T3)−O−Si(T3)−O−Si(T2)	449.7	0.6[b]	−110.9	147.5	0.3
Si(T3)−O−Si(T3)−O−Si(T2)	450.3			147.8	
H(T3)−O−Si(T3)−O−Si(T2)	449.0	1.3[b]	−110.2	147.0	0.8
Al(T3)−O−Si(T3)−O−Al(T2)	488.1	2.4[c]		144.2	1.4
Si(T3)−O−Si(T3)−O−Al(T2)	490.5			145.6	
H(T3)−O−Si(T3)−O−Al(T2)	487.6	2.9[c]		145.7	−0.1
Al(T3)−O−Si(T2)−O−Si(T1)	449.4	0.8[b]	−110.7	147.5	0.3
Si(T3)−O−Si(T2)−O−Si(T1)	450.2			147.8	
H(T3)−O−Si(T2)−O−Si(T1)	450.1	0.1[b]	−111.4	147.7	0.1
Al(T3)−O−Si(T2)−O−Al(T1)	487.6	1.1[c]		145.2	0.2
Si(T3)−O−Si(T2)−O−Al(T1)	488.7			145.4	
H(T3)−O−Si(T2)−O−Al(T1)	489.9	−1.2[c]		145.6	−0.2
Al(T3)−O−Si(T3)−O−Si(T3)	448.7	1.5[b]	−110.0	147.0	0.7
Si(T3)−O−Si(T3)−O−Si(T3)	450.2			147.7	
H(T3)−O−Si(T3)−O−Si(T3)	449.1	1.1[b]	−110.4	146.9	0.8
Al(T3)−O−Si(T3)−O−Al(T3)	486.9	2.9[c]		143.4	2.1
Si(T3)−O−Si(T3)−O−Al(T3)	489.8			145.5	
H(T3)−O−Si(T3)−O−Al(T3)	491.1	−1.3[c]		143.1	2.4
Al(T1)−O−Si(T2)−O−Si(T2)	449.3	0.9[b]	−110.6	147.4	0.5
Si(T1)−O−Si(T2)−O−Si(T2)	450.2			147.9	
H(T1)−O−Si(T2)−O−Si(T2)	450.1	0.1[b]	−111.4	148.2	−0.3
Al(T1)−O−Si(T2)−O−Al(T2)	489.8	0.2[c]		144.8	0.8
Si(T1)−O−Si(T2)−O−Al(T2)	490.0			145.6	
H(T1)−O−Si(T2)−O−Al(T2)	489.6	0.4[c]		144.1	1.5
Al(T1)−O−Si(T3)−O−Si(T3)	448.2	2.3[b]	−109.2	146.9	1.0
Si(T1)−O−Si(T3)−O−Si(T3)	450.5			147.9	
H(T1)−O−Si(T3)−O−Si(T3)	449.4	1.1[b]	−110.4	147.3	0.6
Al(T1)−O−Si(T3)−O−Al(T3)	487.6	2.2[c]		144.5	1.2
Si(T1)−O−Si(T3)−O−Al(T3)	489.8			145.7	
H(T1)−O−Si(T3)−O−Al(T3)	493.4	−3.6[c]		147.5	−1.8
Al(T1)−O−Si(T2)−O−Si(T3)	449.0	0.5[b]	−111.0	147.5	0.2
Si(T1)−O−Si(T2)−O−Si(T3)	449.5			147.7	
H(T1)−O−Si(T2)−O−Si(T3)	449.0	0.5[b]	−110.0	147.3	0.4
Al(T1)−O−Si(T2)−O−Al(T3)	490.5	0.5[c]		145.2	0.2
Si(T1)−O−Si(T2)−O−Al(T3)	491.0			145.4	
H(T1)−O−Si(T2)−O−Al(T3)	490.0	1.0[c]		144.7	0.7

[a] The ^{29}Si chemical shifts were obtained by a conversion of the GIAO shieldings using the calculated and measured shielding/shift values of 450.2 ppm and −111.5 ppm, respectively, for the chabazite sample. $^{29Si}\delta = -111.5 + \Delta(\text{shieldings})$. [b] A positive value indicates a downshift of the corresponding ^{29}Si chemical shift of the *Si* atom present in the Al−O−Si−O−*Si* or H−O−Si−O−*Si* sequences with respect to the ^{29}Si chemical shift of *Si* in Si−O−Si−O−*Si*. [c] A positive value indicates an increase of the corresponding ^{27}Al isotropic chemical shift of the *Al* atom present in the Al−O−Si−O−*Al* or H−O−Si−O−*Al* sequences with respect to the ^{27}Al isotropic chemical shift of *Al* in Si−O−Si−O−*Al*. A negative value reveals the corresponding decrease.

TABLE 6: ^{27}Al NMR Shieldings (ppm) and Average Al(1)−O−T and Al(2)−O−T Angles (deg) for Al of Selected Al(1)−O−Al(2) Sequences

sequence	shielding		Δ[a]	T−O−T	T−O−T	Δ
Al(T2)−O−Al(T2)	481.4	483.3		142.3	143.7	
Al(T2)−O−Si(T2)	490.7		9.3	145.5		3.2
Si(T2)−O−Al(T2)		490.8	7.5		145.5	1.8
Al(T2)−O−Al(T1)[b]	483.3	483.6		141.9	142.7	
Al(T2)−O−Si(T1)	490.2		6.9	145.2		3.3
Si(T2)−O−Al(T1)		491.0	7.4		146.0	3.3
Al(T2)−O−Al(T1)[b]	483.2	483.9		145.7	146.0	
Al(T2)−O−Si(T1)	491.3		8.1	145.4		−0.3
Si(T2)−O−Al(T1)		491.3	7.4		145.9	−0.1

[a] A positive value indicates an increase of the corresponding ^{27}Al isotropic chemical shift of the *Al* atom present in Al−O−*Al* sequences with respect to the ^{27}Al isotropic chemical shift of *Al* in Si−Si−*Al*. [b] These two sequences have symmetrically inequivalent oxygen atoms.

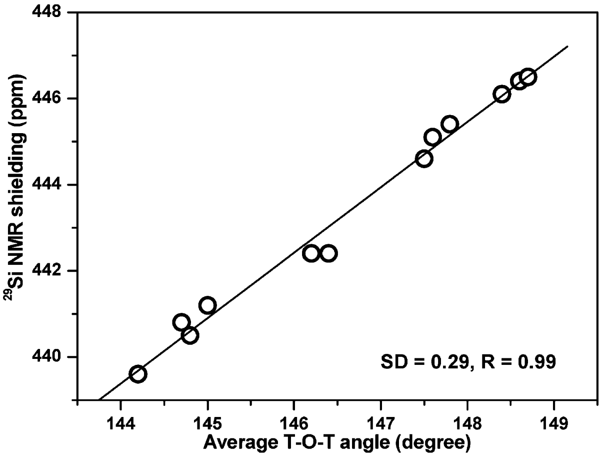

Figure 11. GIAO ^{29}Si NMR shielding values plotted against the average T−O−T angles for the calculated Al−O−*Si* sequences.

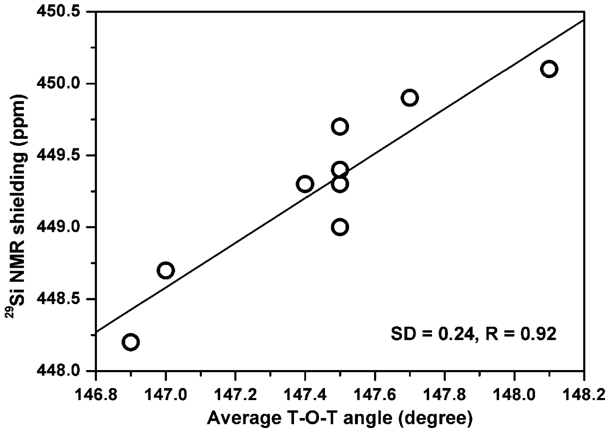

Figure 12. GIAO ^{29}Si NMR shielding values plotted against the average T−O−T angles for the calculated Al−O−Si−O−*Si* sequences.

is possible under specific synthetic conditions but only for the high aluminum framework of the mineral of bicchulite.[64]

In this paper, we employ calculations to estimate the local geometry of AlO_4^- and the ^{27}Al isotropic chemical shift of Al in hypothetical Al−O−Al chains. Our results show that a formation of Al−O−Al sequences in the zeolite framework would be easily recognizable in ^{27}Al (MQ) MAS NMR spectra since the ^{27}Al isotropic chemical shift of Al(3Si,1Al) in Al−O−Al is significantly larger by 7−9 ppm than that of Al(4Si,0Al) (Table 6), leading to values above 67 ppm for Al(3Si,1Al). This change of the ^{27}Al isotropic chemical shift is significantly larger than that caused by a formation of Al−O−(Si−O)$_n$−Al sequences in CHA ($n = 1$) and ZSM-5[27] ($n = 1$ and 2). Therefore, ^{27}Al MQ MAS NMR spectroscopy

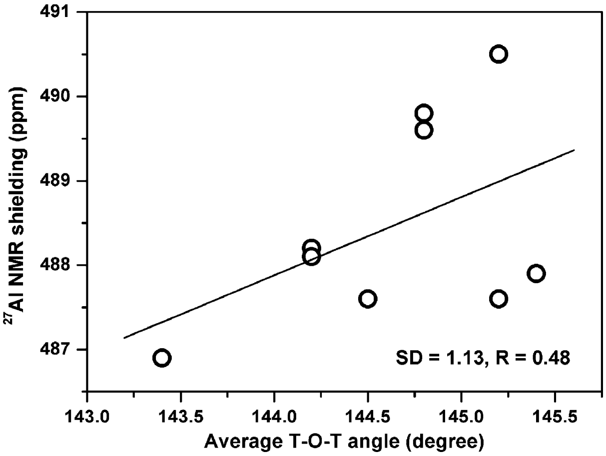

Figure 13. GIAO ^{27}Al NMR shielding values plotted against the average T−O−T angles for the calculated Al−O−Si−O−*Al* sequences.

represents a tool for testing the validity of the Loewenstein rule in matrices with Si/Al > 1. To the best of our knowledge, ^{27}Al resonances above 67 ppm have not been reported in zeolitic materials. This indicates that, even with new methods allowing the preparation of zeolites with rare structures and/or structures with specific framework, the varied Al contents are not conducive to the formation of Al−O−Al sequences in the framework.

7. Conclusions

Our QM-Pot calculations show that Al atoms can occupy three different crystallographic T sites in the framework of the silicon-rich zeolite of the chabazite structure. This result is in agreement with two observed ^{27}Al NMR resonances at 60.0 and 59.2 ppm. The calculated ^{27}Al NMR shielding of 490.0 ppm and the observed ^{27}Al isotropic chemical shift of 60.0 ppm can be used as a secondary internal standard to convert the calculated ^{27}Al NMR shieldings into ^{27}Al isotropic chemical shifts for silicon-rich zeolites.

The calculated downshift by 4−11 ppm of the ^{29}Si chemical shift of Si(3Si,1Al) atoms caused by the effect of Al as a nearest neighbor is in good accord with the experimental values and evidence that the downshift observed in silicon-rich frameworks vary significantly (depending on the zeolite framework) compared to that of Al-rich materials. The effect of more distant Al atoms (Al−O−Si−O−*Si* sequence) is less pronounced (a downshift up to 2 ppm). Both AlO_4^- and SiO_4 local geometries as well as ^{27}Al isotropic and ^{29}Si chemical shifts are significantly affected by the presence of a silanol “nest” (a vacant T site) as a nearest neighbor. Our QM-Pot results reveal a systematic downshift by 11−16 ppm for the ^{29}Si chemical shift of Si(3Si,OH).

Our investigations show that the effects of Al as well as a silanol group (OH) as nearest and next-nearest neighbors on the ^{29}Si chemical shift are always systematic downshifts. Also the influence of Al in Al−O−Si−O−*Al* leads to systematically larger ^{27}Al isotropic chemical shifts of *Al*. On the other hand, there is no systematic contribution of a silanol group in H−O−Si−O−*Al* to the ^{27}Al isotropic chemical shift of *Al*: not even the direction can be predicted without explicit DFT calculations of each chain.

Our results show that the change of the ^{29}Si chemical shift caused by the presence of an Al atom or a silanol group (OH) as a nearest neighbor can reach somewhat larger values compared to the values reported. The change of the local SiO_4 geometry and the ^{29}Si chemical shift depend on the site of the perturbed and perturbing species in the zeolite framework T sites. Weaker but still non-negligible changes were observed for Al and OH as next-nearest neighbors.

Our predictions of NMR parameters using the QM-Pot approach and our bare zeolite framework model (no countercations; no water molecules) are in good agreement with experiments. We conclude that this approach can be successfully employed to propose realistic local structures of AlO_4^- and SiO_4 tetrahedra in silicon-rich zeolite-based catalysts and to interpret their ^{27}Al and ^{29}Si MAS NMR spectra.

Acknowledgment. This work was financially supported by the Grant Agency of the Academy of Sciences of the Czech Republic (Projects No. IAA400400812, IAA400400908, and IAA400400904), the Grant Agency of the Czech Republic (Project No. 203/09/1627), the Academy of Sciences of the Czech Republic (Project No. KAN100400702), and Center of Excellence IDECAT NMP3-CT-2005-011730. We would like to thank Prof. Joachim Sauer and Dr. Blanka Wichterlova for helpful discussions.

Supporting Information Available: The Cartesian coordinates with T site designations of the most stable structure of chabazite (Si/Al = 47) optimized at QM-Pot. This material is available free of charge via the Internet at http://pubs.acs.org.

References and Notes

(1) Corma, A.; Martinez, A. *Catal. Rev.* **1993**, *35*, 483.
(2) Wichterlova, B. *Top. Catal.* **2004**, *28*, 131.
(3) Yahiro, H.; Iwamoto, M. *Appl. Catal., A* **2001**, *222*, 163.
(4) Panov, G. I.; Sheveleva, G. A.; Kharitonov, A. S.; Romannikov, V. N.; Vostrikova, L. A. *Appl. Catal., A* **1992**, *82*, 31.
(5) Newsam, J. M. *J. Phys. Chem.* **1985**, *89*, 2002.
(6) van Bokhoven, J. A.; Koningsberger, D. C.; Kunkeler, P.; van Bekkum, H.; Kentgens, A. P. M. *J. Am. Chem. Soc.* **2000**, *122*, 12842.
(7) Lippmaa, E.; Magi, M.; Samoson, A.; Tarmak, M.; Engelhardt, G. *J. Am. Chem. Soc.* **1981**, *103*, 4992.
(8) Engelhardt, G.; Radeglia, R. *Chem. Phys. Lett.* **1984**, *108*, 271.
(9) Thomas, J. M. *Philos. Trans. R. Soc. London, Ser. A* **1984**, *311*, 271.
(10) Thomas, J. M.; Klinowski, J.; Ramdas, S.; Hunter, B. K.; Tennakoon, D. T. B. *Chem. Phys. Lett.* **1983**, *102*, 158.
(11) Lippmaa, E.; Samoson, A.; Magi, M. *J. Am. Chem. Soc.* **1986**, *108*, 1730.
(12) Engelhardt, G.; Lohse, U.; Lippmaa, E.; Tarmak, M.; Magi, M. *Z. Anorg. Allg. Chem.* **1981**, *482*, 49.
(13) MacKenzie, K. J. D.; Smith, M. E. *Multinuclear Solid-State NMR of Inorganic Materials*, Pergamon: Oxford, U.K., 2002.
(14) Melchior, M. T.; Vaughan, D. E. W.; Jacobson, A. J. *J. Am. Chem. Soc.* **1982**, *104*, 4859.
(15) Engelhardt, G.; Lohse, U.; Patzelova, V.; Magi, M.; Lippmaa, E. *Zeolites* **1983**, *3*, 233.
(16) Debras, G.; Nagy, J. B.; Gabelica, Z.; Bodart, P.; Jacobs, P. A. *Chem. Lett.* **1983**, 199.
(17) Klinowski, J.; Fyfe, C. A.; Gobbi, G. C. *J. Chem. Soc., Faraday Trans.* **1985**, *81*, 3003.
(18) Wolinski, K.; Hinton, J. F.; Pulay, P. *J. Am. Chem. Soc.* **1990**, *112*, 8251.
(19) Bussemer, B.; Schroder, K. P.; Sauer, J. *Solid State Nucl. Magn. Reson.* **1997**, *9*, 155.
(20) Schroder, K. P.; Sauer, J. *J. Phys. Chem.* **1996**, *100*, 11043.
(21) Bull, L. M.; Bussemer, B.; Anupold, T.; Reinhold, A.; Samoson, A.; Sauer, J.; Cheetham, A. K.; Dupree, R. *J. Am. Chem. Soc.* **2000**, *122*, 4948.
(22) Bull, L. M.; Cheetham, A. K.; Anupold, T.; Reinhold, A.; Samoson, A.; Sauer, J.; Bussemer, B.; Lee, Y.; Gann, S.; Shore, J.; Pines, A.; Dupree, R. *J. Am. Chem. Soc.* **1998**, *120*, 3510.
(23) Profeta, M.; Mauri, F.; Pickard, C. J. *J. Am. Chem. Soc.* **2003**, *125*, 541.
(24) Kučera, J.; Nachtigall, P. *Microporous Mesoporous Mater.* **2005**, *85*, 279.
(25) Sklenak, S.; Dedecek, J.; Li, C. B.; Wichterlova, B.; Gabova, V.; Sierka, M.; Sauer, J. *Angew. Chem., Int. Ed.* **2007**, *46*, 7286.

(26) Sklenak, S.; Dedecek, J.; Li, C. B.; Wichterlova, B.; Gabova, V.; Sierka, M.; Sauer, J. *Phys. Chem. Chem. Phys.* **2009**, *11*, 1237.

(27) Dedecek, J.; Sklenak, S.; Chengbin, L.; Wichterlova, B.; Gabova, B.; Brus, J.; Sierka, M.; Sauer, J. *J. Phys. Chem. C* **2009**, *113*, 1447.

(28) Sklenak, S.; Dedecek, J.; Li, C. B.; Gao, F.; Jansang, B.; Boekfa, B.; Wichterlova, B.; Sauer, J. *Collect. Czech. Chem. Commun.* **2008**, *73*, 909.

(29) Loewenstein, W. *Am. Mineral.* **1954**, *39*, 92.

(30) Smith, J. V.; Glasser, L. S. D.; Rinaldi, F. *Acta Crystallogr.* **1963**, *16*, 45.

(31) Zones, S. I. U.S. Patent 4 544 538, 1985.

(32) Zhu, Q.; Kondo, J. N.; Tatsumi, T.; Inagaki, S.; Ohnuma, R.; Kubota, Y.; Shimodaira, Y.; Kobayashi, H.; Domen, K. *J. Phys. Chem. C* **2007**, *111*, 5409.

(33) Zhu, Q. J.; Kondo, J. N.; Ohnuma, R.; Kubota, Y.; Yamaguchi, M.; Tatsumi, T. *Microporous Mesoporous Mater.* **2008**, *112*, 153.

(34) Alemany, L. B. *Appl. Magn. Reson.* **1993**, *4*, 179.

(35) Eichler, U.; Kolmel, C. M.; Sauer, J. *J. Comput. Chem.* **1997**, *18*, 463.

(36) Sierka, M.; Sauer, J. *J. Chem. Phys.* **2000**, *112*, 6983.

(37) Brandle, M.; Sauer, J. *J. Am. Chem. Soc.* **1998**, *120*, 1556.

(38) Eichkorn, K.; Treutler, O.; Ohm, H.; Haser, M.; Ahlrichs, R. *Chem. Phys. Lett.* **1995**, *240*, 283.

(39) Eichkorn, K.; Treutler, O.; Ohm, H.; Haser, M.; Ahlrichs, R. *Chem. Phys. Lett.* **1995**, *242*, 652.

(40) Eichkorn, K.; Weigend, F.; Treutler, O.; Ahlrichs, R. *Theor. Chem. Acc.* **1997**, *97*, 119.

(41) Haser, M.; Ahlrichs, R. *J. Comput. Chem.* **1989**, *10*, 104.

(42) Treutler, O.; Ahlrichs, R. *J. Chem. Phys.* **1995**, *102*, 346.

(43) Gale, J. D. *J. Chem. Soc., Faraday Trans.* **1997**, *93*, 629.

(44) Gale, J. D.; Rohl, A. L. *Mol. Simul.* **2003**, *29*, 291.

(45) Becke, A. D. *Phys. Rev. A* **1988**, *38*, 3098.

(46) Lee, C. T.; Yang, W. T.; Parr, R. G. *Phys. Rev. B* **1988**, *37*, 785.

(47) Miehlich, B.; Savin, A.; Stoll, H.; Preuss, H. *Chem. Phys. Lett.* **1989**, *157*, 200.

(48) Schafer, A.; Huber, C.; Ahlrichs, R. *J. Chem. Phys.* **1994**, *100*, 5829.

(49) Catlow, C. R. A.; Dixon, M.; Mackrodt, W. C. *Lect. Notes Phys.* **1982**, *166*, 130.

(50) Sierka, M.; Sauer, J. *Faraday Discuss.* **1997**, *106*, 41.

(51) Frisch, M. J.; et al. *Gaussian 03*, Revision C.02; Gaussian, Inc.: Wallingford, CT, 2004.

(52) Diaz-Cabanas, M. J.; Barrett, P. A.; Camblor, M. A. *Chem. Commun.* **1998**, 1881.

(53) Fyfe, C. A.; Gobbi, G. C.; Murphy, W. J.; Ozubko, R. S.; Slack, D. A. *J. Am. Chem. Soc.* **1984**, *106*, 4435.

(54) Fyfe, C. A.; Gobbi, G. C.; Kennedy, G. J. *J. Phys. Chem.* **1984**, *88*, 3248.

(55) Thomas, J. M.; Klinowski, J. *Adv. Catal.* **1985**, *33*, 199.

(56) Kuehl, G. H.; Timken, H. K. C. *Microporous Mesoporous Mater.* **2000**, *35−6*, 521.

(57) van Bokhoven, J. A.; Roest, A. L.; Koningsberger, D. C.; Miller, J. T.; Nachtegaal, G. H.; Kentgens, A. P. M. *J. Phys. Chem. B* **2000**, *104*, 6743.

(58) Grobet, P. J.; Geerts, H.; Martens, J. A.; Jacobs, P. A. *J. Chem. Soc., Chem. Commun.* **1987**, 1688.

(59) Grobet, P. J.; Jacobs, P. A.; Beyer, H. K. *Zeolites* **1986**, *6*, 47.

(60) Magi, M.; Lippmaa, E.; Samoson, A.; Engelhardt, G.; Grimmer, A. R. *J. Phys. Chem.* **1984**, *88*, 1518.

(61) Engelhardt, G.; Lohse, U.; Samoson, A.; Magi, M.; Tarmak, M.; Lippmaa, E. *Zeolites* **1982**, *2*, 59.

(62) Stach, H.; Janchen, J.; Jerschkewitz, H. G.; Lohse, U.; Parlitz, B.; Zibrowius, B.; Hunger, M. *J. Phys. Chem.* **1992**, *96*, 8473.

(63) Johnson, G. M.; Mead, P. J.; Dann, S. E.; Weller, M. T. *J. Phys. Chem. B* **2000**, *104*, 1454.

(64) Dann, S. E.; Mead, P. J.; Weller, M. T. *Inorg. Chem.* **1996**, *35*, 1427.

JP9042232